THE SURFACE CONTACT OF VISCOELASTIC MATERIALS. PART I – ALGORITHM OVERVIEW

Sergiu Spinu[1,2], Delia Cerlinca[1,2]

[1] *Department of Mechanics and Technologies, Stefan cel Mare University of Suceava, 13th University Street, 720229, Romania, e-mail: sergiu.spinu@fim.usv.ro, delia@fim.usv.ro*
[2] *Integrated Center for Research, Development and Innovation in Advanced Materials, Nanotechnologies, and Distributed Systems for Fabrication and Control (MANSiD), Stefan cel Mare University, Suceava, Romania.*

Abstract: *The difficulty in solving the viscoelastic contact problem stems from two facts: (1) both contact area and pressure distribution are a priori unknown, and (2) the contact parameters keep changing with time even when the load is kept constant. These drawbacks are overcome in this paper by conducting numerical analysis based on both spatial and temporal model discretization. The spatial discretization allows for the iteration of the contact area and of its related pressure distribution, whereas the additional temporal discretization provides ground for the evaluation of the time-dependent response of the viscoelastic material. The contact process is simulated by computing a series of contact states, in which every new state is assessed based on information derived in all previous states. The numerical predictions agree well with the classic solution of the spherical contact undergoing a step loading. The algorithmic computational efficiency is discussed, and a mesh convergence study in the temporal dimension is conducted.*

Keywords: *numerical simulation, viscoelastic contact, viscoelastic displacement*

1. Introduction

The service life of machine elements made by viscoelastic matrix can be extended considerably by improving their tribological performance. The mathematical modelling of viscoelastic behavior in the frame of contact mechanics requires simplifying assumptions, such as linearity or incompressibility, and solutions in the literature are limited to particular geometries (sphere, cone) or to viscoelastic models with only one relaxation time. The numerical analysis can overcome this issues, and therefore has become the subject of numerous research efforts [1-3].

The classic solutions [4-8] in literature of the linear viscoelastic contact are based on the correspondence principle between the elastic and the viscoelastic problems of stress analysis. The latter principle allows the direct implementation of elastic solutions in the viscoelastic problems, provided the boundary conditions are properly handled. In the case of the contact problem, the changing boundary conditions limit the applicability of the correspondence principle. Initial contact solutions [4-6] for the contact radius obtained in this way are subjected to limited applicability related to the monotony of the contact radius. These limitations were gradually released [7-9], but the contact problem must remain axisymmetric. The latter condition might not be satisfied in case of surface contacts undergoing eccentric loading.

In the numerical algorithm developed herein, the technique of deriving the viscoelastic solution from its elastic counterpart is applied to displacement computation instead of the contact radius. The contact area and the pressure distribution are assessed by means of a contact solver whose convergence was previously discussed [10].

The resulting contact model can simulate the contact behavior of linear viscoelastic materials with arbitrary contact geometry, arbitrary loading history, and complex rheological behavior.

2. Discrete contact model

The contact problem is described in a Cartezian coordinate system with the x_1 and x_2 axes laying in the common plane of contact, i.e. the plane that separates best the limiting surfaces of the contacting bodies. Based on the framework developed in [11], the frictionless contact problem can be reduced to a model consisting in three type of equations: (1) the equation of the surface of deformation between the two bodies, (2) the boundary conditions, and (3) the static equilibrium. As this paper deals with the surface (i.e. conforming) contact, the static force equilibrium equations are completed with the torque equations, meaning the force can be applied eccentrically with respect to contact normal axis x_3. Without losing generality, the eccentricity is allowed along the x_1-axis in the current model, leading to a tilting moment about the x_2-axis.

The geometry of the contact problem yields the following condition of deformation, expressing the clearance between the contacting bodies:

$$h(x_1, x_2) = hi(x_1, x_2) + u_3(x_1, x_2) - \omega_3(t) - \alpha(t)x_1,$$
$$(x_1, x_2) \in \Gamma, \tag{1}$$

where h denotes the gap between the deformed bodies, hi the initial gap (in unloaded state), u_3 the composite (i.e., relative) displacement along the x_3-axis, ω_3 the rigid-body approach, α the tilting angle due to the normal force eccentricity, and Γ the considered computational domain, expected to include the contact region.

The boundary conditions and constraints are related to the assumptions of (1)

non-negativity of pressure and (2) impenetrability of the bodies in the frame of Linear Theory of Elasticity. The first assumption leads to neglect of contact adhesion, and can be considered very conservative in the case of adhesive contacting material; however, this assumption is required to obtain the pressure distribution by the classic minimization process seeking the minimum of a quadratic form, as described in [10]. It should be noted that this assumption is common in the literature of the viscoelastic contact. The second assumption involves the non-negativity of the clearance between the contacting surfaces:

$$p(x_1, x_2) \geq 0, \, h(x_1, x_2) \geq 0, \, (x_1, x_2) \in \Gamma. \tag{2}$$

With the additional constraints that pressure is nil outside the contact area, and the clearance is nil on the contact area, the boundary conditions can be expressed as:

$$p(x_1, x_2)h(x_1, x_2) = 0, \, (x_1, x_2) \in \Gamma. \tag{3}$$

The static equilibrium provides additional equations constraining the unknown pressure distribution:

$$W = \iint_{\Gamma} p(x_1, x_2)dx_1dx_2 \, ; \tag{4}$$

$$We = \iint_{\Gamma} p(x_1, x_2)x_1dx_1dx_2 \, , \tag{5}$$

where W denotes the normal load, and e its eccentricity (i.e., the distance to the contact normal axis).

The difficulty in solving the contact model (1) - (5) stems from the fact that neither the contact area, nor the pressure distribution are known in advance. An iterative approach is therefore needed, involving a trial-and-error approach, in which a contact region is assumed, and the pressure distribution is then computed based on this assumption. If all constraints in the contact model are verified by the obtained solution, the contact problem solution is achieved. This solution is unique based on the theorem of uniqueness of solution

of the elastostatic problem. Otherwise, the contact area is adjusted and a new pressure distribution is computed with the new guess. This iterative approach requires that the response of the contacting material, i.e. the displacement induced by the surface tractions, is computed for arbitrary contact area and pressure distribution. The latter computation can only be achieved numerically, and therefore a spatial discretization is imposed to perform the numerical analysis of the contact process.

A rectangular uniform mesh, having $N_1 \times N_2$ grids, is established in the common plane of contact, with its sides aligned with the axes of the coordinate system. A representative point (usually the center) is chosen for each elementary cell, and all problem parameters are assumed piecewise-constant, based on the discrete values computed in the control points. The notation of problem parameters can then make use of the discrete indexes of the elementary cells instead of the continuous coordinates in the analytical model.

The main advantage is the substitution of integration of arbitrary functions over arbitrary domains with summation, as discussed in the following section.

3. Viscoelastic displacement computation

In case of an elastic material of shear modulus G and Poisson's ratio ν, by adopting the half-space approximation authorizing the use of the Boussinesq solution for a point force acting on the half-space boundary, the displacement u_3^{el} results as:

$$u_3^{el}(x_1, x_2) = \int_{-\infty}^{\infty} \int_{-\infty}^{\infty} B(x_1 - x_1', x_2 - x_2') \times$$
$$p(x_1', x_2') dx_1' dx_2', \tag{6}$$

where $B(x_1, x_2) = (1-\nu) / (2\pi G \sqrt{x_1^2 + x_2^2})$ is the displacement induced at a point of coordinates (x_1, x_2) by a unity normal concentrated force acting in origin.

Based on the spatial discretization discussed in the previous section, the numerical counterpart of Eq. (6) results as:

$$u_3^{el}(i, j) = \sum_{k=1}^{N_1} \sum_{\ell=1}^{N_2} K_{el}(i-k, j-\ell) p(k, \ell),$$
$$i = 1 \ldots N_1, j = 1 \ldots N_2, \tag{7}$$

where K_{el} is the elastic influence coefficient, i.e. the integral of $B(x_1, x_2)$ over the elementery cell of side lengths Δ_1 and Δ_2 along directions of $\vec{x}_1$ and $\vec{x}_2$, respectively:

$$K_{el}(i-k, j-\ell) =$$
$$\int_{x_2(\ell)-\Delta_2/2}^{x_2(\ell)+\Delta_2/2} \int_{x_1(k)-\Delta_1/2}^{x_1(k)+\Delta_1/2} B(x_1(i) - x_1', x_2(j) - x_2') dx_1' dx_2' \tag{8}$$

The influence coefficient $K_{el}(i-k, j-\ell)$ expresses the normal displacement induced in the cell (i, j) by a uniform pressure of magnitude $1/(\Delta_1 \Delta_2)$ Pa acting in the cell (k, ℓ).

The viscoelastic response in the frame of linear viscoelasticity can be described with the aid of two interchangeable functions, namely the creep compliance function $\Phi(t)$, expressing the strain response to a unit step change in stress, and/or the relaxation modulus $\Psi(t)$, expressing the stress response to a unit step change in strain. By applying superposition in the Boltzmann hereditary integral $\int_0^t () dt'$, the viscoelastic response, strain or stress, to any sequence of stress or strain, respectively, can be obtained.

Based on the correspondence principle between the elastic and the viscoelastic solution of a problem of stress analysis, Lee and Radok [4] obtained the contact radius in the viscoelastic spherical contact problem by applying the hereditary integral to the Hertz solution, in which the elastic contact compliance $1/(2G)$ was replaced by the viscoelastic creep compliance. The same technique can be applied to Eq. (6), leading to

the viscoelastic displacement induced by a history of pressure $p(x_1', x_2', t')$ in a window of observation $[0, t]$, under the assumption that prior to time $t = 0$ the body was undisturbed:

$$u_3^{vs}(x_1, x_2, t) = 2G \int_0^t \Phi(t - t') \frac{\partial}{\partial t'} u_3^{el}(x_1, x_2) dt' . \quad (9)$$

Interchanging differentiation and integration in Eq. (9) yields:

$$u_3^{vs}(x_1, x_2, t) = 2G \int_0^t \int_{-\infty}^{\infty} \int_{-\infty}^{\infty} \Phi(t - t') \times$$

$$B(x_1 - x_1', x_2 - x_2') \frac{\partial p(x_1', x_2', t')}{\partial t'} dx_1' dx_2' dt' . \quad (10)$$

Whereas Eq. (6) requires a spatial discretization only to achieve the computation of displacement induced by an arbitrary pressure distribution, Eq. (10) implies integration over the loading history, which can be achieved by imposing an additional temporal discretization. To this end, the loading window $[0, t]$ is divided into small time steps, and the problem parameters are assumed piecewise-constant in the time dimension as well. The derivative of pressure is further on approximated by the finite difference $p(i, j, k) - p(i, j, k-1)$, and the Boltzmann hereditary integral is substituted by the summation operator, leading to the following numerical counterpart of the continuous equation (10):

$$u_3^{vs}(i, j, k) = \sum_{n=1}^{N_t} \sum_{\ell=1}^{N_1} \sum_{m=1}^{N_2} K_{vs}(i - \ell, j - m, k - n) \times$$

$$\left(p(\ell, m, n) - p(\ell, m, n-1) \right),$$

$$i = 1 \dots N_1, j = 1 \dots N_2, k = 1 \dots N_t, \quad (11)$$

where $K_{vs}(i - \ell, j - m, k - n)$ is the viscoelastic influence coefficient, expressing the displacement induced after k time steps in the spatial cell (i, j), by a uniform pressure of magnitude $1/(\Delta_1 \Delta_2)$ Pa, that acted in the cell

(ℓ, m) in the nth time step of the observation window, with $n \le k$.

The relation between the elastic and the viscoelastic influence coefficient was derived in [12]:

$$K_{vs}(i, j, k) = 2G\Phi(k)K_{el}(i, j) . \quad (12)$$

The integration of the viscoelastic displacement equation (11) in the contact model (1) - (5) is discussed in the following section.

4. Algorithm overview

Equation (11) clearly shows that, in order to compute the displacement at a time t in the observation window, the entire history of pressure distribution in the viscoelastic contact is needed. Therefore, the contact model (1) - (5) needs to be solved successively at every time step, thus assuring the simulation of the loading history.

The flow chart of the proposed algorithm is presented in Fig. 1, in which an upper index was used to denote the temporal step. In the beginning of the observation window, as there is no loading history, the contact problem is solved as a purely elastic process, i.e. the displacement is generated by the current pressure only. In the subsequent time increments, the computed pressure history is superimposed in the displacement equation, as if the contact has a modified initial contact geometry hi. With this approach, the type of algorithm employed [13] to solve the frictionless elastic contact problem can be used for the viscoelastic contact simulation.

The algorithmic computational complexity is dictated by the number of cells in the spatial mesh, i.e. $N_1 \times N_2$, as well as by the number of temporal steps N_t.

The most computationally intensive operations are the convolution products related to the superposition of pressure effects in the two spatial dimensions. The computational impact is dramatic because these convolutions must be computed [13] two times per iteration.
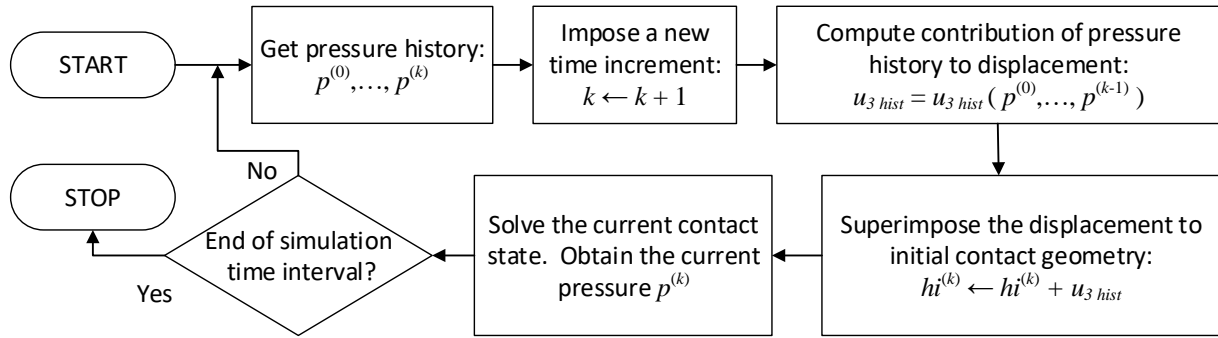
Figure 1: Algorithm flowchart

The calculation can be accelerated by employing the FFT assisted convolution computation [14], so that the order of operations is decreased from $O(N_1^2 N_2^2)$ to $O(N_1 N_2 \log(N_1 N_2))$ per time step.

The overall order of computations is $O(N_t^2 N_1 N_2 \log(N_1 N_2))$, suggesting that a fine temporal discretization might increase considerably the computational requirements. In our contact simulations, convergence was reached even with a relatively small number of time increments, as shown in the following section.

5. Program validation

The computer program was first benchmarked against purely elastic analytical solutions for the surface circular contact under eccentric loading. When the normal load is applied eccentrically, the contact problem is no longer axisymmetric, and the number of closed-form solution in the literature is limited to a few. The validation of the contact solver was achieved against the solution advanced by Lur'e [15], as shown in Fig. 2, under the assumption that the force eccentricity e, defined as ratio to the indenter radius R, is small enough so that the contact does not open (i.e. the contact area remains circular). The latter assumption, valid for minute tilting angles, is released with the current numerical formulation, which can predict contact opening without additional difficulty, as shown in Fig. 3. It should also be noted that the analytical pressure distribution in Fig. 2 tends to infinity at the indenter edge, as a result of the ordinate discontinuity. This theoretical behavior can only partially be reproduced by the numerical approach, as the latter employs averaging of pressure on the cells of the computational domain.
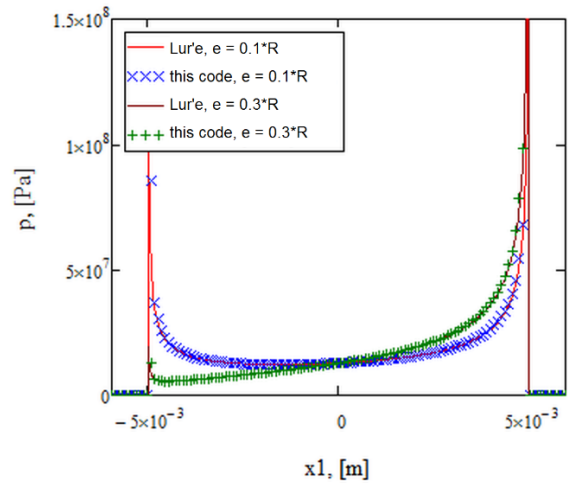
Figure 2: Comparison of pressure distributions in the plane $x_2 = 0$, various eccentricities
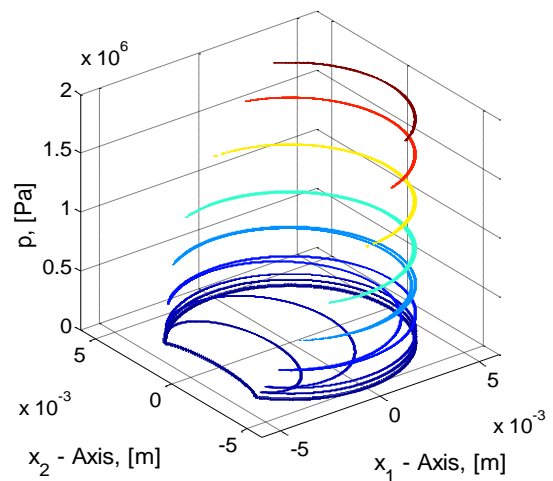
Figure 3: Prediction of contact opening due to eccentric loading

A second contact scenario involves the concentrated axisymmetric contact of viscoelastic materials whose constitutive law is described by basic rheological models. The implicit solutions derived in the classical literature [7,8] of the viscoelastic contact for the Maxwell and Zener units, brought to a more computationally friendly form for the step loading $W(t) = W_0 H(t)$ by Ciornei [16], were taken as reference for the numerical predictions of the newly developed computer program. The Hertz contact parameters (contact radius a_H, central pressure p_H), were used as normalizers in Figs. 4 and 5, depicting the pressure distributions achieved at various time moments from the loading history. The relevant formulas [16] used in the generation of the reference data are given in Table 1. In both cases, the contact radius can be expressed as: $a(t) = \sqrt[3]{3RW_0\Phi(t)/8}$.

The numerical simulation was conducted by imposing a 256×256 spatial mesh and 100 temporal steps, resulting in the pressure distributions depicted using continuous lines in Figs. 4 and 5. The data computed numerically according to Table 1 is also displayed as reference, using dashed lines.

Rheological model	Creep compliance	Radial pressure distribution
Maxwell $\eta \quad G$	$\Phi(t) = \dfrac{1}{2G}\left(1 + \dfrac{t}{\tau}\right),$ $\tau = \eta/G$	$p(t,r) = \dfrac{8G}{\pi R}\left(\left(a(t)^2 - r^2\right)^{\frac{1}{2}} - \dfrac{1}{\tau}\int_0^t \exp\left(\dfrac{t'-t}{\tau}\right)\mathrm{Re}\left(\left(a(t')^2 - r^2\right)^{\frac{1}{2}}\right)dt'\right)$
Zener η_K G G_K	$\Phi(t) = \dfrac{1}{2}\left(\dfrac{1}{G} + \dfrac{1 - e^{-\frac{t}{\tau}}}{G_K}\right),$ $\tau = \eta_K/G_K$	$p(t,r) = \dfrac{8G}{\pi R}\left(\left(a(t)^2 - r^2\right)^{\frac{1}{2}} - \dfrac{1}{\tau}\int_0^t \exp\left(\dfrac{2(t'-t)}{\tau}\right)\mathrm{Re}\left(\left(a(t')^2 - r^2\right)^{\frac{1}{2}}\right)dt'\right)$
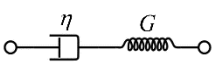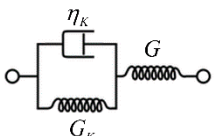
Table 1: The solution for the viscoelastic spherical contact for basic rheological models
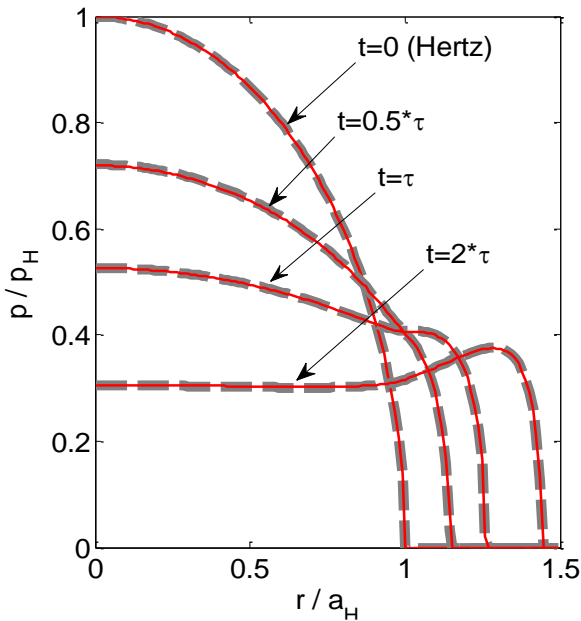
Figure 4: Pressure history, Maxwell model
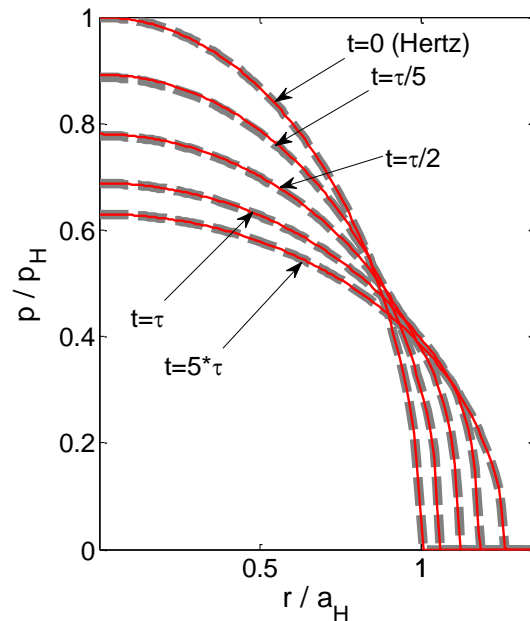
Figure 5: Pressure history, Zener model

In an additional simulation, a temporal mesh convergence study is performed, consisting in a gradual refining of the mesh in the temporal dimension. The pressure distributions predicted for the same time moment, obtained with the same spatial discretization but with various number of temporal steps, are compared in Fig. 6. The numerical simulations suggest that mesh convergence can be achieved with a relatively small number of time steps, and consequently the contact process can be simulated with reduced computational resources for a long observation window.
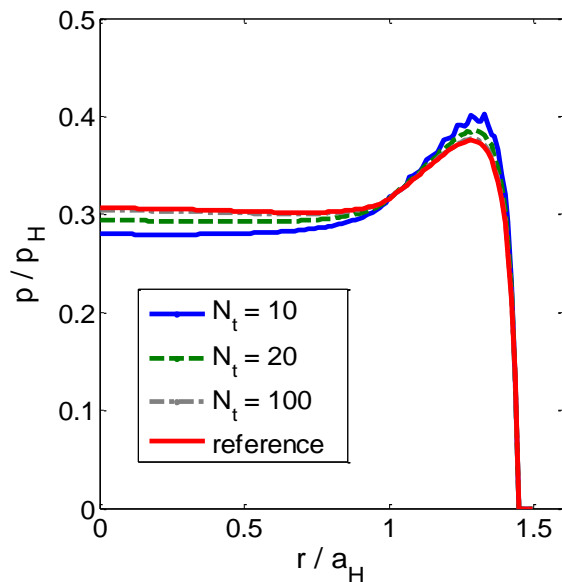
Figure 6: Mesh convergence, Maxwell model, $t = 2\tau$

6. Conclusions

An algorithm for the simulation of the conforming contact of viscoelastic materials is advanced in this paper, by joining a versatile solver for the frictionless normal contact with a numerical technique to achieve the linear viscoelastic displacement of the surface subjected to a known but arbitrary distribution of pressure. The latter method is based on the elastic-viscoelastic correspondence principle, sanctioning the use of solutions of elastic problems of stress analysis to derive the viscoelastic solutions of the associated viscoelastic problems.

The contact solver requires spatial discretization to assess the pressure distribution and the contact area in an iterative manner, provided the response of the contacting material is known. The computation of viscoelastic displacement necessitates an additional temporal discretization, and the current displacement is computed based on the entire history of the contact loading. Consequently, the viscoelastic contact process simulation is achieved by computing a series of subsequent contact states, in which the current state is based on information from all previous states.

The employed contact solver is well adapted to conforming contact scenarios, in which the normal force may be applied eccentrically, resulting in the tilting of the common plane of contact. Compared to existing analytical results, the algorithm can predict large tilting angles leading to contact opening.

Program validation is achieved by comparison with existing results for the Hertz spherical contact of viscoelastic materials modeled by basic rheological models of linear viscoelasticity.

The strong points of the newly advanced computer program consist in: (1) the ability to incorporate complex models of viscoelasticity (including the ones in discrete form as resulting from experimental measurements) involving more than one relaxation time, (2) the capability of the contact solver to treat arbitrary (not only axisymmetric) contact geometry, and (3) the capacity to simulate arbitrary loading histories.

7. Acknowledgement

8. References

[1] Chen, W. W., Wang, Q. J., Huan, Z., and Luo, X., 2008, *Semi-Analytical Viscoelastic Contact Modeling of Polymer-Based Materials*, ASME J. Tribol., **133**(4), 041404 (10 pages).

[2] Kozhevnikov, I. F., Duhamel, D., Yin, H. P., and Feng, Z.-Q., 2010, *A New Algorithm for Solving the Multi-Indentation Problem of Rigid Bodies of Arbitrary Shapes on a Viscoelastic Half-Space*, Int. J. Mech. Sci., **52**(3), pp. 399-409.

[3] Spinu, S., 2015, *Numerical Simulation of Viscoelastic Contacts. Part 1. Algorithm Overview*, J. Balk. Tribol. Assoc., **21**(2), pp. 269-280.

[4] Lee, E. H., and Radok J. R. M, 1960, *The Contact Problem for Viscoelastic Bodies*, ASME J. Appl. Mech., **27**(3), pp. 438-444.

[5] Hunter, S. C., 1960, *The Hertz Problem for a Rigid Spherical Indenter and a Viscoelastic Half-Space*, J. Mech. Phys. Solids, **8**(4), pp. 219-234.

[6] Yang, W. H., 1966, *The Contact Problem for Viscoelastic Bodies*, ASME J. Appl. Mech., **33**(2), pp. 395-401.

[7] Ting, T. C. T., 1966, *The Contact Stresses Between a Rigid Indenter and a Viscoelastic Half-Space*, ASME J. Appl. Mech., **33**(4), pp. 845-854.

[8] Ting, T. C. T., 1968, *Contact Problems in the Linear Theory of Viscoelasticity*, ASME J. Appl. Mech., **35**(2), pp. 248-254.

[9] Greenwood, J. A., 2010, *Contact between an Axisymmetric Indenter and a Viscoelastic Half-Space*, Int. J. Mech. Sci., **52** (6), p. 829.

[10] Kalker, J. J., Van Randen, Y. A., 1972, *A Minimum Principle for Frictionless Elastic Contact with Application to Non-Hertzian Half-Space Contact Problems*, J. Eng. Math., **6** (2), p. 193.

[11] *Johnson*, K. L., 1985, *Contact Mechanics*, Cambridge University Press, Cambridge.

[12] Spinu, S., and Gradinaru, D., 2015, Semi-*Analytical Computation of Displacement in Linear Viscoelastic Materials*, IOP Conf. Ser.: Mater. Sci. Eng. **95**, 012111 (7 pages).

[13] Polonsky, I. A., and Keer L. M., 1999, *A Numerical Method for Solving Rough Contact Problems Based on the Multi-Level Multi-Summation and Conjugate Gradient Techniques*, Wear, **231**(2), pp. 206-219.

[14] Liu, S. B., Wang, Q., and Liu, G., 2000, *A* Versatile *Method of Discrete Convolution and FFT (DC-FFT) for Contact Analyses*, Wear, **243**(1-2), pp. 101-111.

[15] Lur'e, A. I., 1964, *Three-Dimensional Problems of the Theory of Elasticity*, Interscience Publishers, translated from Russian.

[16] Ciornei, F. C., 2004, *On the Hertzian Circular Dynamic Contact in the Linear Viscoelastic Domain*, Ph.D. Thesis (in Romanian), University of Suceava, Romania.